X-RAY RADIOGRAPHY: A NEW TECHNIQUE FOR MEASURING DIFFUSION COEFFICIENTS IN ROCK SAMPLES

Lisa Cavé, Yan Xiang & Tom Al
Geology Department – University of New Brunswick, Fredericton, New Brunswick, Canada
Peter Vilks
Atomic Energy of Canada Limited, Pinawa, Manitoba, Canada
Monique Hobbs
Ontario Power Generation, Toronto, Ontario, Canada

ABSTRACT
A non-destructive X-ray radiography technique has been developed for measuring diffusion coefficients in sedimentary rock samples. Changes in X-ray absorption are used to quantify concentration changes as iodide tracer diffuses through rock pores. Pore water diffusion coefficients (D_p) are obtained by fitting an analytical solution to the concentration profiles. Mean pore water diffusion coefficients were measured for Queenston Formation shale (5.0×10^{-11} $m^2.s^{-1}$) and Cobourg Formation limestone (2.5×10^{-11} $m^2.s^{-1}$) and compared with through diffusion results. Both methods gave similar pore water (D_p) and effective (D_e) diffusion coefficient values.

RÉSUMÉ
Une technique de radiographie au rayon X a été développée pour mesurer les coefficients de diffusion dans des échantillons de roches. L'adsorption de rayon X est utilisée pour quantifier les variations de la concentration d'un tracer, l'iode, diffusant dans les pores. Les coefficients de diffusions de l'eau des pores (D_p) sont obtenus en simulant les profiles de concentration par une solution analytique. Les coefficients de diffusion moyens de l'eau dans les pores pour des échantillons de la formation de schistes de Queenston (5.0×10^{-11} $m^2.s^{-1}$) et la formation de calcaire de Cobourg (2.5×10^{-11} $m^2.s^{-1}$) ont été mesurés et comparé avec les mesures de la technique de la "through-diffusion".

1 INTRODUCTION

Diffusion is expected to be the dominant mechanism of solute transport in rock materials surrounding a deep geologic repository (DGR) in low permeability sedimentary rocks. Determining the diffusion properties of sedimentary rocks is therefore an important component of site characterization activities. Laboratory measurement techniques, based on the principles of Fick's laws, are most often employed for the determination of diffusion coefficients for rock samples (Shackelford 1991). The measurements typically involve monitoring the flux of a tracer solute that diffuses into, out of, or through, the sample under conditions where the fluid velocity is zero. For through-diffusion, in-diffusion and out-diffusion methods, standard analytical chemical techniques are used to quantify solute concentration changes over time in solution reservoirs connected to the sample. Diffusion coefficients can also be determined by fitting a solution of Fick's Second Law to a tracer concentration profile developed across the sample during a diffusion test. This may require sectioning the sample to extract the tracer solute and determine the concentrations.

In this study, an X-ray radiography method has been developed for characterizing and quantifying iodide tracer concentration profiles in a rock sample during diffusion tests. Unlike sectioning techniques, the X-ray measurements are non-destructive, allowing repeat time series measurements to be made on the same sample. The method also has the advantage over steady-state though-diffusion methods in that data are collected before the tracer breaks through the sample. This can represent a significant saving in experimental time, especially for relatively thick samples of low permeability materials.

Here we describe the methods for preparing samples, conducting iodide tracer diffusion tests, collecting radiographic time series data and analyzing the data to generate pore water diffusion coefficients (D_p) for iodide in rock samples. Methodology testing was conducted using archived core samples of Queenston Formation shale and Cobourg Formation limestone from southern Ontario, Canada. Results from X-ray radiographic measurements are compared to results from conventional through-diffusion techniques conducted on adjacent samples.

2 BACKGROUND

2.1 X-ray techniques for measuring rock properties

One of the earliest reported uses of X-ray techniques in diffusion studies was the investigation of rubidium diffusion profiles in soils using X-ray autoradiography of an ^{86}Rb tracer (Evans and Barber 1964). Since then, X-ray radiography techniques using iodide as a tracer have been applied to various problems in the geologi-

cal sciences, e.g. measuring spatially distributed saturation fields (Tidwell and Glass 1994); investigating spatial variations in porosity and diffusion in dolomite (Tidwell et al. 2000); and studying heterogeneous diffusion in fractured crystalline rocks (Altman et al. 2004). Three dimensional X-ray computed tomography (CT) techniques have also been employed to characterize phase distributions of pore fluids and minerals; pore geometry (van Geet et al. 2001, Císlerová and Votrubová 2002) and iodide tracer diffusion in various types of rock (Polak et al. 2003, Zhelezny and Shapiro 2006).

Techniques for measuring solute tracer concentrations in rocks are based on the principle of X-ray attenuation, which increases predictably with increasing concentration of an X-ray attenuating tracer in the rock sample according to the Beer-Lambert Law:

$$I = I_0 \exp(-\mu d) \quad [1]$$

where: I_0 is the intensity of an X-ray beam incident on the sample; I is the intensity of the transmitted X-ray beam, which is attenuated during transmission through the sample; d is the thickness (or path length) through the sample and μ is the attenuation coefficient. The attenuation coefficient depends on the X-ray energy, the electron density of the sample and the chemical composition of the substance (van Geet et al. 2001). At constant energy, the attenuation coefficient increases with increasing atomic number, which makes high atomic number elements, such as iodide, suitable for use as tracers in X-ray radiography. In this study, potassium iodide (KI) solutions have been used as the tracer. Although the potassium ions do make some contribution to the X-ray attenuation, their effect is small compared to the attenuation by iodide, because of their lower atomic number.

Individual attenuation coefficients are difficult to define for geological samples which are inherently heterogeneous, because the X-ray beam typically passes through several materials of differing thickness, density and composition in the sample. For geologic materials containing fluid-filled pores, μ may be defined as:

$$\mu = (1 - \Phi)\cdot\mu_m + \Phi\cdot\mu_p \quad [2]$$

where μ_m is the absorption coefficient for the solid material; μ_p is the absorption coefficient for the pores and Φ is a porosity term. To overcome this problem, a blank subtraction approach may be used (e.g., Tidwell et al. 2000, Altman et al. 2004), whereby time series radiographs (samples with tracer) are subtracted from a reference radiograph (sample without tracer). This approach is taken for the method described in this paper.

Referring to Eq. 2, μ_m is constant throughout the diffusion experiment but μ_p changes in response to the changing tracer concentration in the pore fluid. Subtracting the time series images from the reference allows the effect of the tracer to be visualized in isolation from the X-ray attenuation effects of the rock matrix. The blank subtraction calculation yields the parameter $(\Delta\mu_p)_{i,j}$ (simplified as Δμ), which represents the change in X-ray attenuation coefficient due to the presence of iodide tracer in the pores at each pixel (i,j) in the time series radiograph images. For a sample of constant thickness, Δμ of the pore water may be defined as:

$$(\Delta\mu_p)_{i,j} = \ln(I_{ref})_{i,j} - \ln(I_t)_{i,j} = (\mu_{p2} - \mu_{p1})_{i,j} \cdot \Phi_{i,j} \quad [3]$$

where: $(I_{ref})_{i,j}$ is the transmitted X-ray intensity at a pixel (i,j) on the reference radiograph and $(I_t)_{i,j}$ is the transmitted X-ray intensity at the same pixel on the time series radiograph, and μ_{p1} and μ_{p2} are the attenuation coefficients of the pore fluids without and with iodide, respectively. The parameter Δμ is a function of the mass of tracer along the X-ray path and can be calibrated to give quantitative measurements of tracer concentration.

2.2 Diffusion measurements

In a porous medium, diffusive transport is constrained within the saturated pore spaces which results in a diminished mass flux compared to a comparable cross section in homogenous solution. The decrease in mass flux is commonly accounted for by the inclusion of the porosity and tortuosity terms in the diffusion coefficient term in Fick's laws

$$D_e = D_0 \cdot \Phi \cdot \tau_f \quad [4]$$

where D_e is the effective diffusion coefficient for a porous medium, D_0 is the free water diffusion coefficient, Φ, a porosity term and τ_f is the tortuosity factor. The free water diffusion coefficient for potassium iodide at infinite dilution at 25°C is 2.045×10^{-9} $m^2.s^{-1}$ (Vanýsek 2006).

The porosity term represents the decrease in cross-sectional area for diffusive transport caused by the presence of mineral grains in the porous medium. The porosity term may be obtained in a variety of ways, each resulting in slightly different values. It is common to use the diffusion accessible porosity (Φ_d) that is obtained from time-lag analysis of steady-state through-diffusion experiments (Shackelford, 1991). In this work, however, we use a water loss porosity (Φ_w) obtained by gravimetric measurement (Emerson, 1990) because it is not possible to obtain the Φ_d term by radiographic measurements. For a conservative solute that is not affected by size exclusion in the pore spaces, the value of Φ_w should approach Φ_d.

The tortuosity factor accounts for the difference between the shortest straight line transport path and the

effective transport path length through the pore network which is tortuous in nature. The tortuosity factor also accounts for the effects of constricted pathways or channels along the diffusion path. The tortuosity factor is dimensionless (≤ 1) and is defined as:

$$\tau_f = \delta \cdot \tau = \frac{\delta}{(L_e / L)^2} \quad [5]$$

where δ is the constrictivity term, L_e and L are the effective and straight-line path lengths, respectively and τ is the tortuosity.

In our experiments, pore water diffusion coefficients (D_p), (which exclude the porosity term) are derived by fitting an analytical solution of Fick's Second Law to one-dimensional concentration versus distance profiles obtained from X-ray radiography diffusion tests. For the appropriate experimental initial conditions:

t = 0: $x \geq 0$, $C_{i(x,t)} = 0$

and boundary conditions:

t > 0: $x = 0$, $C_{i(x,t)} = C_0$ $x = L$, $C_{i(x,t)} = 0$

the analytical solution is (Crank, 1975):

$$C_{i(x,t)} = C_0 \, \mathrm{erfc} \frac{x}{2\sqrt{D_p t}} \quad [6]$$

where: C_i is the concentration of tracer at a distance x from the diffusion boundary at time t since the start of diffusion; C_0 is the concentration of tracer at the influx boundary; L is the height of the sample and erfc is the complimentary error function. The pore water diffusion coefficient is related to the effective diffusion coefficient by the expression:

$$D_p = \frac{D_e}{\phi_w} \quad [7]$$

3 RADIOGRAPHY METHOD

The X-ray radiography method provides a non-destructive means of monitoring the diffusive transport of an iodide tracer through a rock sample. The technique is a modification of the X-ray absorption imaging reported by Tidwell et al. (2000) and Altman et al. (2004) using iodide tracers in geologic materials.

The X-ray method was tested with diffusion measurements made on archived core samples of shale (Queenston Formation) and limestone (Cobourg Formation) from southern Ontario. To enable a comparison with an accepted benchmark, measurements were also made on adjacent core samples using conventional through-diffusion cells, using a method similar to that of Boving and Grathwohl (2001).

3.1 Synthetic pore water

Pore water composition data from crush and leach experiments were used to formulate synthetic pore water, with which the samples were saturated prior to diffusion. The synthetic pore water was used as a matrix for the iodide tracer solution in order to maintain geochemical equilibrium and minimize reactions between minerals and solutions that might affect the porosity and hence the diffusive properties. The iodide tracer was prepared by substituting molar concentrations of KI for NaCl in the solutions to produce the same ionic strength as the synthetic pore water, thereby avoiding osmotic pressure effects.

3.2 Sample preparation

Diffusion experiments were conducted on cylindrical rock cores (11 mm diameter, 20 mm length) mounted vertically in aluminum diffusion cells (Fig. 1), designed to fit the sample holder of a Skyscan 1072 desktop X-ray micro computed tomography system (microCT). Aluminum was chosen for the cell material because of its low atomic number, which leads to low absorption and scattering of the X-rays. The cores were cut from larger drill core samples with a diamond-tipped core bit (Technodiamant) using kerosene or water circulated through the bit as cooling fluid. Paired samples were prepared to investigate anisotropy by cutting the cylinder axes of the cores normal (NB) and parallel (PB) to the bedding planes of the sedimentary rock. After oven-drying, the cores were coated around the circumference with epoxy (Presi Mecaprex MA2), leaving the top and bottom faces uncoated to allow for contact with the solutions. The ends of the cores were positioned in the aluminum reservoirs and sealed with epoxy. An internal standard and alignment guide, in the form of a small wire or flat metal sheet of aluminum, was attached vertically to the side of the core.

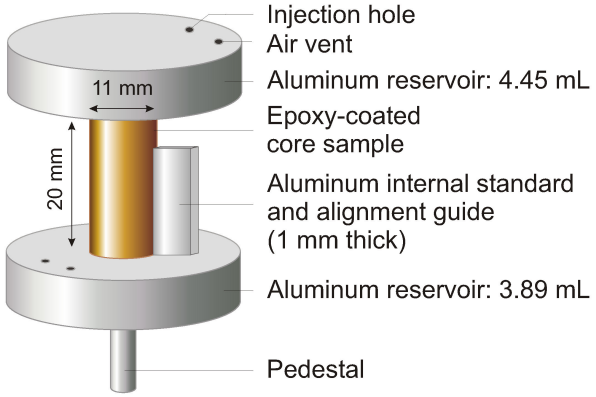

Figure 1. X-ray radiography diffusion cell.

The diffusion cells with attached rock cylinders were submerged in synthetic pore water under vacuum for 2 to 5 weeks to saturate the samples before collecting the initial reference radiographs. After saturation, the diffusion cell reservoirs were capped and sealed with electrical tape. Injection holes in the caps were used to ensure that the reservoirs remained full throughout the diffusion test and between injections the holes were covered with tape. Diffusion cells were stored under saturated humidity at 22±1°C.

3.3 Quantification of pore iodide concentrations

Two approaches were used to quantify the iodide concentration in the pores in the time series radiographs during the diffusion experiments. We have termed these the relative approach and calibrated approach.

The relative approach measures relative tracer concentrations C/C_0 as a function of distance from the source of the tracer, using a final X-ray radiograph collected when all the pores in a sample are fully saturated with the tracer solution. The equation for deriving relative concentration values at each point in the data set is (Tidwell and Glass 1994):

$$\left(\frac{C}{C_0}\right)_{i,j} = \frac{\ln(I_t)_{i,j} - \ln(I_r)_{i,j}}{\ln(I_s)_{i,j} - \ln(I_r)_{i,j}} \qquad [8]$$

where: C is the concentration at pixel (i,j); C_0 is the tracer concentration at the influx boundary; and I is the measured (transmitted) X-ray intensity at pixel (j,j); with the subscripts t, r and s indicating the time series, reference (zero tracer) and tracer-saturated radiograph images, respectively.

In all images, the properties of the solid rock matrix remain constant for each pixel on the radiograph. In the tracer-saturated image, the concentration of the tracer in the pore spaces is also constant, therefore the Δμ values at each pixel are a function of porosity. The value of C/C_0 at any point is determined by:

$$C/C_0 = \Delta\mu_t/\Delta\mu_s \qquad [9]$$

An alternative approach is the calibrated approach, in which the absolute concentration of iodide in the pores in the time series images is determined from a calibration curve. A multi-point calibration curve for Δμ versus iodide concentration (Fig. 2) is derived from measurements made on standard potassium iodide solutions in glass vials having a comparable diameter (11 mm) to the core samples. The calibration standards were prepared in a synthetic pore water matrix and blank subtraction was used to remove the effects of the glass and synthetic pore water to generate Δμ values that are a function of the iodide concentration in solution.

Iodide concentrations calculated from the Δμ values measured during the diffusion tests are divided by the Φ_w values to convert from measurements of total iodide mass in the rock to pore solution iodide concentrations. The pore iodide concentration values are then normalized by the known concentration of the iodide tracer at the influx boundary to give C/C_0.

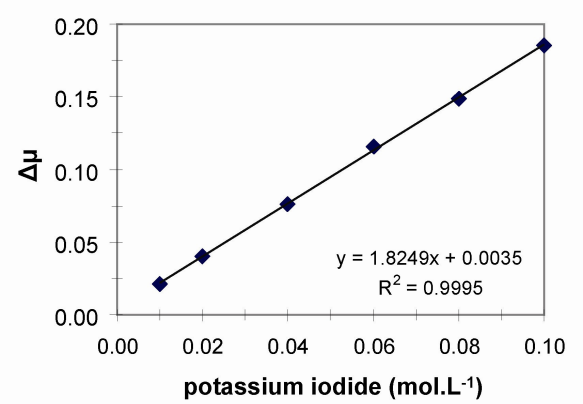

Figure 2. A calibration curve for standard potassium iodide in synthetic pore water.

3.4 Diffusion tracer experiments and data collection

Diffusion experiments were conducted on rock samples using X-ray radiography to make periodic measurements of the iodide tracer distribution along the direction of diffusion in the sample. Transmission radiographs were generated using the microCT system. Radiographs were collected in digital format using a cone beam X-ray source, operated at 60kV and 164 μA, and an X-ray scintillation detector optically coupled to a CCD camera. A 1-mm aluminum filter was inserted between the source and the sample to filter out low energy X-ray radiation from the source. Eight data frames were collected and averaged for each radiograph, using an acquisition time of 8 seconds per frame. Radiographs were saved as 1024 × 1024 pixel 16 bit greyscale TIFF images with a spatial resolution of 18.7 × 18.7 $\mu m^2.pixel^{-1}$. The 16 bit format allows for 65536 distinct greyscale values at each pixel, representing a measure of the transmitted X-ray intensity (I). A mechanically operated sample stage in the microCT, and rotation alignment guides on the samples, were used to position the sample in the same location and orientation for successive radiograph acquisitions, allowing for blank subtraction of time series images. Consistent instrumental settings were used for all reference and time series images.

Reference images (sample blanks) were collected after 2 to 5 weeks of saturation, with the reservoirs filled with synthetic pore water. The diffusion experiments were then started by replacing the synthetic pore water solution in the lower reservoir with iodide tracer solution. Initial tracer concentrations of 0.6, 0.8 and 1.0 $mol.L^{-1}$

KI were used for experiments on Queenston Formation shale; and 1.0 mol.L^{-1} KI for Cobourg Formation limestone samples. Higher concentrations of iodide are preferred because they increase the absorption and improve signal to noise ratios. When replacing the solutions, fresh tracer was injected slowly by syringe (1 to 2 mL.min^{-1}) into the bottom of the lower reservoir. Paper towel was used to wick the displaced solution away from the air vent hole. The volume injected was at least 3 to 5 times the total volume of the reservoir to ensure that the previous solution was completely flushed out. The cells were then sealed, rinsed and dried and the time of the initial tracer injection marked on the diffusion cell as the start time, t = 0.

The upper reservoirs remained filled with synthetic pore water to maintain a zero-iodide boundary condition through the diffusion phase of the experiments. The tracer solution in the lower reservoirs was refreshed regularly (every 3 to 5 days) in an attempt to maintain a constant iodide concentration at the influx boundary. Radiographs were collected at increasing time intervals as the tracer diffused upwards.

When image processing revealed that the iodide tracer had broken through to the upper reservoir, the synthetic pore water in the upper reservoir was also replaced with iodide tracer solution and the samples allowed to saturate completely with iodide from both ends. During the iodide saturation phase, the solutions in both reservoirs were refreshed approximately weekly. Radiograph images were also collected at 1-week intervals to monitor the progress of iodide saturation and the final iodide-saturated images collected when no further changes were observed.

3.5 Radiography data processing

Radiograph images were processed with ImageJ v 1.36, a java-based open-source image processing application developed by the National Institutes of Health (Rasband 2006). The step-by-step procedure is illustrated in Fig. 3.

Corresponding reference- and time series images were cropped to an identical region of interest (ROI) over the rock sample before analysis (Step 1). Radiograph greyscale values were averaged over each row of pixels in the cropped images to produce a profile of mean greyscale intensity versus distance along the diffusion pathway (Step 2). In this way, the two dimensional radiographs were condensed to one-dimensional profiles, removing the effect of the cylindrical sample geometry (i.e. variable X-ray path length across the width of the sample). The averaging approach also compensates for small errors in the sample alignment.

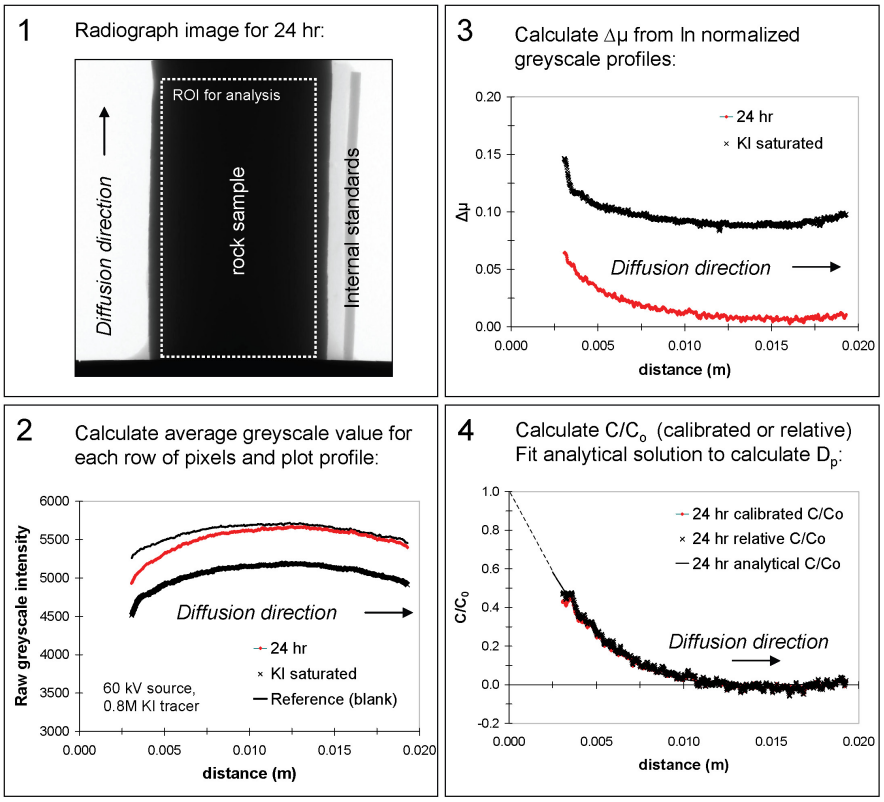

Figure 3. Procedure for determining pore water diffusion coefficients (D_p) from radiography data. An example is given for the 24 hour time series radiograph from shale sample QA105PB with 0.8 mol.L^{-1} potassium iodide tracer in synthetic pore water solution. Note that the data set is rotated 90° between Step 1 and Step 2 to simplify plotting.

Mean greyscale values for the aluminum internal standard were used to normalize the data for each time series profile relative to the reference profile, in order to correct for minor fluctuations in the X-ray source between radiograph acquisitions. Profiles of $\Delta\mu$ were calculated according to Eq. 3 (Step 3).

Profiles of relative iodide concentrations (C/C_0) could then be obtained following either of the two approaches outlined in Section 3.3. Finally, analytical solutions for Fick's Second Law were modelled using Eq. 6 and plotted with the C/C_0 versus distance data for each time step. Iterative adjustment of the estimated value of D_p allowed us to find a curve that closely matched the observed diffusion profiles for each time step before tracer breakthrough (Step 4).

3.6 Through-diffusion experiments

Measurements of D_e were made using conventional through-diffusion cells for comparison of the radiography results with an accepted benchmark. Rock core slices of diameter 47 to 85 mm and length 10 mm were mounted vertically in the diffusion cells between two reservoirs of equal hydraulic head. Sodium iodide tracer (0.06 mol.l^{-1} or 1 mol.l^{-1}) was added to one of the reservoirs to establish a concentration gradient and the diffusive flux of iodide through the sample into the elution reservoir was measured with an iodide selective electrode. Values of D_e and Φ_d were determined from the iodide mass flux after steady-state was reached, using the method described by van Loon et al. (2003) and gravimetric Φ_w used to calculate D_p using Eq. 7.

4 RESULTS AND CONCLUSIONS

The results of the radiographic measurements are presented in Table 1. For each sample, the pore diffusion coefficient (D_p) for the last time step before tracer breakthrough is reported. Examples of blank subtracted time series radiographs for one of the limestone samples are also shown in Fig. 4, illustrating the transport of iodide through the sample. Through-diffusion measurements for adjacent samples are reported in Table 2.

In general, limestone samples have slightly lower porosities and diffusion coefficients for iodide than the shale samples, although the D_p values for all samples were of the same order of magnitude (10^{-11} m^2.s^{-1}). Some of the limestone samples present challenges to the analytical sensitivity of the radiography measurements, because of very low porosity (0.01 to 0.03) and strong X-ray absorbing properties of the Ca-rich rock.

The heterogeneous distribution of porosity in the Cobourg limestone samples is also a complicating factor. The calibrated technique and D_p calculations require knowledge of the material porosity. But the bulk Φ_w measurement made on an adjacent core segment may not necessarily have the same porosity as the diffusion test sample. Below about 3% water loss porosity, the detection sensitivity of the iodide tracer in the rock is also poor and the height of the C/C_0 versus distance curve, which is sensitive to the porosity value, may not be sufficiently different from the background. Sample heterogeneity may be responsible for the large range of D_p and D_e values obtained for the limestone samples by the through-diffusion technique.

Table 1. Iodide pore water- and effective diffusion coefficients measured by radiography for shale and limestone.

Sample identifier	Pore water D_p (m^2.s^{-1})	Effective D_e (m^2.s^{-1})	Tortuosity factor	Φ_w	KI concentration at inlet (mol.L^{-1})
Q078NB1	7.5×10^{-11}	4.6×10^{-12}	0.044	0.062	0.6
Q078NB2	4.0×10^{-11}	2.5×10^{-12}	0.022		0.6
Q078NB3	8.0×10^{-11}	4.9×10^{-12}	0.039		1.0
Q078NB4	5.0×10^{-11}	3.1×10^{-12}	0.027		1.0
Q105NB1	2.0×10^{-11}	1.2×10^{-12}	0.010	0.059	0.8
Q105PB1	3.0×10^{-11}	1.8×10^{-12}	0.015		0.8
Shale av ± s.d.	**$(5.0 \pm 2.4) \times 10^{-11}$**	**$(3.1 \pm 1.5) \times 10^{-12}$**	**0.026**	**0.060**	**0.6 - 1.0**
C036NB1	4.0×10^{-11}	1.2×10^{-12}	0.020	0.030	1.0
C036PB1	2.0×10^{-11}	6.1×10^{-13}	0.010		1.0
C036NB2	2.5×10^{-11}	7.5×10^{-13}	0.012		1.0
C036PB2	2.5×10^{-11}	7.5×10^{-13}	0.012		1.0
C036NB3	2.5×10^{-11}	7.4×10^{-13}	0.012		1.0
C036PB3	1.5×10^{-11}	4.4×10^{-13}	0.007		1.0
Limestone av ± s.d.	**$(2.5 \pm 0.8) \times 10^{-11}$**	**$(7.5 \pm 2.6) \times 10^{-13}$**	**0.012**	**0.030**	**1.0**

Note: Sample identifiers indicate rock formation (Q = Queenston, C = Cobourg); 078 = depth below surface (in metres); NB = normal to bedding, PB = parallel to bedding. Final digit denotes replicate samples. Other symbols: av. = arithmetic mean; s.d. = standard deviation.

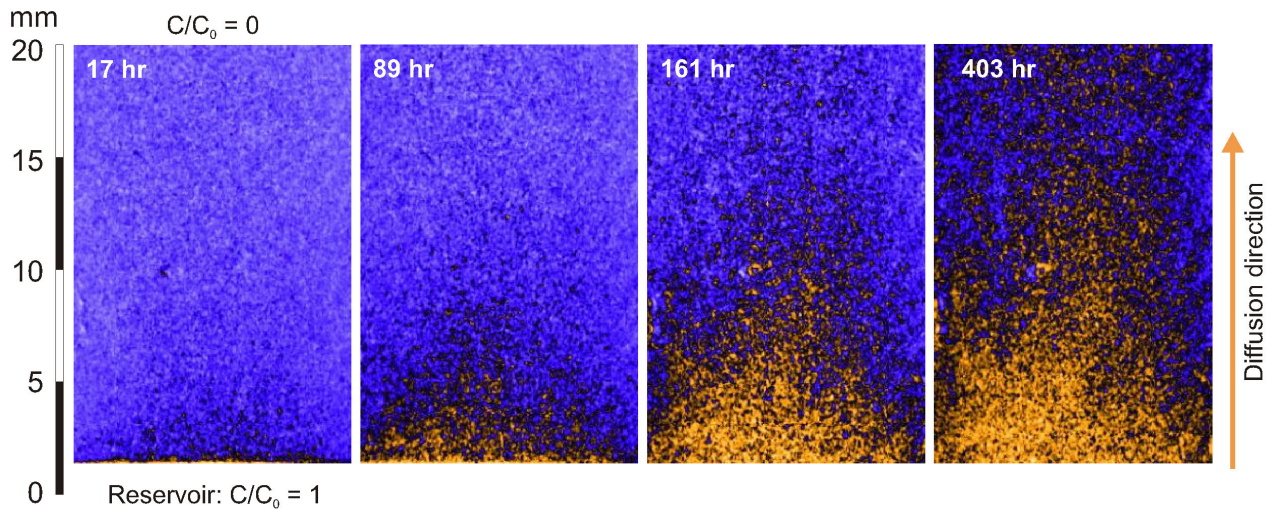

Figure 4. Examples of blank subtracted radiographs for 4 time steps during diffusion of 1.0 mol.L^{-1} potassium iodide tracer into a limestone sample. The tracer breaks through to the upper diffusion boundary after 161 hours.

Table 2. Through-diffusion pore water- and effective diffusion coefficients for shale and limestone samples.

Sample identifier	Pore water D_p (m^2.s^{-1})	Effective D_e (m^2.s^{-1})	Φ_w	Φ_d	NaI concentration at inlet (mol.L^{-1})
Q078NB1	1.9×10^{-11}	1.3×10^{-12}		0.041	0.06
Q078NB2	2.5×10^{-11}	1.7×10^{-12}		0.045	0.06
Q084NB	1.6×10^{-11}	1.0×10^{-12}		0.049	0.06
Q089NB1	3.7×10^{-11}	2.4×10^{-12}		0.036	1.0 (KI)
Q089NB2	3.9×10^{-11}	2.6×10^{-12}	0.066	0.031	1.0 (KI)
Q105NB1	1.3×10^{-11}	8.7×10^{-13}		0.029	0.06
Q105NB2	1.7×10^{-11}	1.1×10^{-12}		0.034	0.06
Q087PB	2.4×10^{-11}	1.6×10^{-12}		0.024	0.06
Q096PB	1.4×10^{-11}	9.4×10^{-13}		0.024	0.06
Shale av ± s.d.	**$(2.3 \pm 1.0) \times 10^{-11}$**	**$(1.5 \pm 0.6) \times 10^{-12}$**	**0.066**	**0.035**	**0.06 – 1.0**
C036NB1	1.2×10^{-11}	2.0×10^{-13}		0.012	0.06
C036NB2	5.6×10^{-12}	9.5×10^{-14}		0.004	0.06
C036NB3	9.4×10^{-12}	1.6×10^{-13}		0.005	0.06
C044NB	2.5×10^{-11}	4.2×10^{-13}	0.017	0.014	0.06
C056NB	2.2×10^{-11}	3.8×10^{-13}		0.011	0.06
C056NB2	8.1×10^{-11}	1.4×10^{-12}		0.030	1.0 (KI)
C056NB3	3.6×10^{-11}	6.2×10^{-13}		0.013	1.0 (KI)
C036PB	1.6×10^{-11}	2.8×10^{-13}		0.015	0.06
Limestone av ± s.d.	**$(3.7 \pm 3.2) \times 10^{-11}$**	**$(6.2 \pm 5.6) \times 10^{-13}$**	**0.017**	**0.013**	**0.06 – 1.0**

Note: Sample identifiers indicate rock formation (Q = Queenston, C = Cobourg); 078 = depth below surface (in metres); NB = normal to bedding, PB = parallel to bedding. Final digit denotes replicate samples. Other symbols: av. = arithmetic mean; s.d. = standard deviation.

Comparing samples prepared for diffusion normal to the bedding planes and those prepared parallel to bedding, it appears that there is no significant effect of anisotropy on the diffusion coefficients obtained by radiography or through-diffusion in this sample set. The small size of the samples does limit the scale of heterogeneity that can be investigated by radiography, however, and most samples were prepared from regions of core with fairly uniform appearance. In this limited data set, the influence of stratigraphic position may be greater than that of orientation for shales. Two deeper shale samples (105 m) had slightly lower D_p values than the shallower samples (78 m) in the radiography data set.

Diffusion coefficients also appear to be insensitive to tracer concentration when using similar high concentrations (0.6 to 1.0 mol.l^{-1}) for radiography. There is greater variation between duplicate samples measured using the same tracer concentration (e.g. Q078NB1 and Q078NB2) than between samples measured with different concentrations of iodide (e.g. Q078NB1 and QA78NB3). All Cobourg limestone radiography samples were measured with a concentrated 1.0 mol.L^{-1} KI solution in an attempt to improve analytical sensitivity. The vastly different tracer concentrations used for through-diffusion experiments (0.06 and 1.0 mol.l^{-1}) do appear to affect the results, with higher values of D_e obtained with the higher tracer concentration tracer.

Comparison of results from the radiography (Table 1) and through-diffusion methods (Table 2) shows similar D_p and D_e values obtained by both techniques. Values of D_p measured for shales are slightly higher (2 to 8 × 10^{-11} m^2.s^{-1}) than those calculated (1.3 to 3.9 × 10^{-11} m^2.s^{-1}) from through-diffusion D_e values. The two samples measured with 1.0 KI mol.l^{-1} tracer give a better comparison, having Dp values at the upper end of the range. Radiography measurements on limestones give D_p values (1.5 to 4.0 × 10^{-11} m^2.s^{-1}) within the range of those calculated from through diffusion data (0.56 to 8.1 × 10^{-11} m^2.s^{-1}). The radiography results were obtained for a 2-cm diffusion path length in under 7 days, while the through-diffusion over a 1-cm path length took 20 to 30 days to reach steady state, highlighting the time saving advantage of radiography.

ACKNOWLEDGEMENTS

Radiography was assisted by John Bowles, Siva Thangavelu and Paul Arsenault of the LTMD X-ray laboratory, Department of Mechanical Engineering, University of New Brunswick.

REFERENCES

Altman, S.J., Uchida, M., Tidwell, V.C., Boney, C.M. and Chambers, B.P. 2004. Use of X-ray absorption imaging to examine heterogeneous diffusion in fractured crystalline rocks. *Journal of Contaminant Hydrology,* 69: 1 - 26.

Boving, T.B. and Grathwohl, P. 2001. Tracer diffusion coefficients in sedimentary rocks: correlation to porosity and hydraulic conductivity. *Journal of Contaminant Hydrology*, 53: 85 - 100.

Císlerová, M. and Votrubová, J. 2002. CT derived porosity distribution and flow domains. *Journal of Hydrology*, 267: 186 - 200.

Crank, J. 1975. *The mathematics of diffusion*, 2nd ed., Clarendon Press, Oxford, UK.

Emerson, D.W. 1990. Notes on mass properties of rocks – density, porosity, permeability. *Exploration geophysics*, 21: 209 - 216.

Evans, S.D. and Barber, S.A. 1964. The effect of cation-exchange capacity, clay content and fixation of rubidium-86 diffusion in soil and kaolinite systems. *Proceedings of the Soil Science Society of America*, 28(1): 53 - 56.

Polak, A., Grader, A.S., Wallach, R. and Nativ, R. 2003. Chemical diffusion between a fracture and the surrounding matrix: Measurement by computed tomography and modeling. *Water Resources Research*, 39(4), 1106, SBH10-1 - SBH10-14.

Rasband, W. 2006. *ImageJ Version 1.36, 13 March 2006. Complete release notes*. National Institutes of Health, USA. Available online at http://rsb.info.nih.gov/ij/.

Shackelford, C.D. 1991. Laboratory diffusion testing for waste disposal – a review. *Journal of Contaminant Hydrology*, 7: 177 - 217.

Tidwell, V.C. and Glass, R.J. 1994. X ray and visible light transmission for laboratory measurement of two-dimensional saturation fields in thin-slab systems. *Water Resources Research*, 30(11): 2873 - 2882.

Tidwell, V.C., Meigs, L.C., Christian-Frear, T. and Boney, C.M. 2000. Effects of spatially heterogeneous porosity on matrix diffusion as investigated by X-ray absorption imaging. *Journal of Contaminant Hydrology*, 42: 285 - 302.

van Geet, M., Swennen, R. and Wevers, M. 2001. Towards 3-D petrography: application of microfocus computer tomography in geological science. *Computers and Geoscience*, 27: 1091 - 1099.

van Loon, L.R, Soler, J.M. and Bradbury, M.H. 2003. Diffusion of HTO, $^{36}Cl^-$ and $^{125}I^-$ in Opalinus Clay samples from Mont Terri. Effect of confining pressure. J*ournal of Contaminant Hydrology*, 61: 73 - 83.

Vanýsek, P. 2006. Ionic conductivity and diffusion at infinite dilution. In Lide, D.R. (ed). *CRC Handbook of Chemistry and Physics.* 87th ed., CRC Press: 5-76 – 5-78.

Zhelezny, P.V. and Shapiro, A.A. 2006. Experimental investigation of the diffusion coefficients in porous media by application of X-ray computer tomography. *Journal of Porous Media*, 9(4): 275 - 288.